INSTITUTE OF PHYSICS PUBLISHING JOURNAL OF PHYSICS B: ATOMIC, MOLECULAR AND OPTICAL PHYSICS

J. Phys. B: At. Mol. Opt. Phys. **34** (2001) 4939–4956 PII: S0953-4075(01)24305-3

Spatial alignment of diatomic molecules in intense laser fields: II. Numerical modelling

E Springate[1], F Rosca-Pruna[1], H L Offerhaus[1], M Krishnamurthy[2] and M J J Vrakking[1]

[1] FOM Institute for Atomic and Molecular Physics, Kruislaan 407, 1098 SJ Amsterdam, The Netherlands
[2] Tata Institute of Fundamental Research, Homi Bhabha Road, Mumbai 400 005, India

Received 26 April 2001, in final form 21 August 2001
Published 26 November 2001
Online at stacks.iop.org/JPhysB/34/4939

Abstract

The angular distributions of ionic fragments produced by multi-electron dissociative ionization of diatomic molecules are calculated using a field-ionization Coulomb explosion model that includes dynamic rotation of the molecule in the laser field. The majority of dynamic alignment occurs on the leading edge of the laser pulse at low intensities before the laser intensity reaches the dissociative ionization threshold. This makes the degree of alignment sensitive to the precise value of the dissociative ionization threshold. Measuring the total ion signal for different pulse-lengths enables angle-dependent dissociative ionization to be distinguished from dynamic alignment. Increased alignment with long pulses is an unambiguous sign that the molecules are forced into alignment with laser field.

1. Introduction

When small molecules irradiated by intense laser pulses fragment through multi-electron dissociative ionization (MEDI), the ions are preferentially ejected along the polarization axis [1]. There has been considerable debate about whether this means that the molecules are aligned prior to or during ionization and dissociation ('dynamic' alignment), or simply whether molecules that are already oriented along the polarization axis are preferentially ionized and dissociated ('geometric' alignment).

Several experiments have been carried out to identify which of these two alignment mechanisms is responsible for the observed anisotropy. Double-pulse experiments, where the molecules were irradiated with two laser pulses with crossed polarizations and a time delay between them, suggested that molecules could be aligned with intense picosecond or femtosecond pulses [2–4]. With circular polarization, molecules align to a plane rather than an axis (the field vector rotates too quickly for a molecule to follow). The differences between the fragmentation patterns obtained with linearly and circularly polarized light can then be

used to evaluate the degree of geometric alignment [5]. The ratio of the ion signals parallel and perpendicular to the polarization axis as a function of intensity has also been used to distinguish dynamic from geometric alignment [6, 7]. In these experiments, an increase in the signal perpendicular to the laser polarization and a broadening of the fragment angular distributions with increasing intensity were taken as the signatures of geometric alignment, as ions further from the polarization axis are ionized at higher intensities. In our group, we have identified our experimental observation of increased alignment of iodine and bromine molecules with increasing laser pulse-length as an indication of the occurrence of dynamic alignment [8].

The field-ionization Coulomb explosion model [6,9,10] has provided theoretical evidence for the importance of geometric alignment. This model, which considers a single outer electron bound by the double-well potential of a diatomic molecule in the laser electric field, predicts lower ionization thresholds for molecules aligned along the laser polarization axis. Once one electron has been removed from the molecule, the two ion cores begin to separate along a dissociative potential curve. Upon the loss of additional electrons, the ions move apart due to their mutual Coulomb repulsion. As the ions move apart, the central barrier between the two ions rises until the outer electron can become localized on one ion core. When this happens, the electron energy is Stark-shifted upwards. This results in a lower ionization threshold for molecules aligned close to the laser polarization axis at a critical internuclear separation, somewhat larger than the equilibrium internuclear separation. This model has been successful in explaining why the ion fragments produced by MEDI of diatomic molecules have lower energies than would be expected from Coulomb explosion at equilibrium separation [10].

Dynamic alignment can occur when the dipole moment induced by the electric field of an intense linearly polarized laser pulse aligns the internuclear axis of a molecule along the laser polarization axis [11]. Classical trajectory calculations of the dynamic alignment of molecules as they ionize and dissociate in intense laser fields have shown that, for light molecules, a substantial degree of alignment can occur even for laser pulses as short as 70–80 fs [2]. Solution of the time-dependent Schrödinger equation has demonstrated that HCN molecules can align on a subpicosecond timescale when irradiated by laser pulses with intensities $\sim 10^{13}$ W cm^{-2} [12]. In contrast to techniques such as hexapole focusing [13] and orientation in a strong DC electric field [14] which are only applicable to polar molecules, this technique is potentially applicable to all molecules with a non-isotropic polarizability. It has recently been demonstrated that it is possible to align all three axes of a molecule along a given space-fixed coordinate frame using elliptically polarized laser fields [15]. The ability to create samples of aligned molecules has a number of important applications. From an aligned sample of molecules, it is possible to measure photoelectron angular distributions in the molecular frame. Enhanced high harmonic generation from aligned molecules has also been observed [16]. For all these potential applications, it is important to establish under what conditions the strong anisotropies in MEDI fragment ion distributions are really due to dynamic alignment of molecules or just a result of the angle-dependent dissociative ionization (geometric alignment).

In this paper, we calculate angular distributions of the ions produced by multi-electron dissociative ionization of molecules. We use a field-ionization Coulomb explosion model [6, 10], extended to two dimensions, and include the effect of the dynamic rotation of the molecule in the laser field. We have investigated the dependence of the degree of alignment on laser intensity and pulse-length, as well as on molecular parameters such as mass, polarizability and dissociative ionization threshold intensity. The angular distributions are compared with those obtained with geometric alignment alone to demonstrate how geometric and dynamic

alignment can be distinguished. The results of these numerical calculations are compared with experimental measurements also carried out by our group, which are described in detail in a companion to this paper [8].

2. Description of the model

The model presented in this paper is a classical calculation of the time evolution of the angular and internuclear coordinates of homonuclear diatomic molecules (I_2 and Br_2) irradiated by intense ($\sim 10^{13}$–10^{15} W cm^{-2}) and short (~ 50 fs–5 ps), linearly polarized laser pulses. In this model, dynamic alignment of the molecules along the laser polarization axis is reflected in the time evolution of the angular coordinate due to the interaction of the laser-induced dipole with the laser field. The time evolution of the radial coordinate reflects the dissociation of the molecule during the multi-electron dissociative ionization process.

Schematically, the calculations (explained in more detail below) proceed as follows: initially the molecule is considered to be at rest at the equilibrium internuclear bond distance, with a given initial angle between the internuclear axis and the laser polarization axis. As the laser turns on, the molecule begins to rotate due to the laser-induced dipole (dynamic alignment). When the laser intensity reaches a critical value, the molecule is ionized, and it is assumed that the molecule is excited to a dissociative curve. From here on the angular and the radial motion are coupled. Now, at each time-step in the calculation we assess whether the outer electron remains bound in the electrostatic potential of the laser electric field and both nuclei. As the shape of the potential energy surface depends on the angle between the internuclear axis and the laser polarization axis, it is responsible for the appearance of geometrical alignment in the calculation. If the electron energy is high enough to pass over the potential barriers, the electron leaves the molecule. The two nuclei then move apart due to their mutual Coulomb repulsion.

At the end of the laser pulse, the trajectory calculation gives the asymptotic recoil angle and the asymptotic charge state. We repeat the calculation for a number of initial angles between the internuclear axis and the laser polarization axis. By properly weighting these results, the calculations can be used to simulate the outcome of recent experiments on the multi-electron dissociative ionization of I_2 and Br_2 performed in this group [8] (see section 3). The remainder of this section is devoted to a more detailed description of the ingredients mentioned above.

2.1. Angular motion (dynamic alignment)

Homonuclear diatomic molecules have no permanent dipole moment and so the angular rotation of the molecule is caused by the dipole moment induced by the laser field. This is also true for molecules that do possess a permanent dipole, as the interaction with a permanent dipole averages to zero over the laser period. The interaction potential with the induced dipole, averaged over the laser period, is given by [11]

$$V(\theta) = -\tfrac{1}{4}\varepsilon_0^2(\alpha_\parallel \cos^2\theta + \alpha_\perp \sin^2\theta). \tag{1}$$

Here, $\alpha_\parallel$ and $\alpha_\perp$ are the polarizability components parallel and perpendicular to the internuclear axis, θ is the angle between the internuclear and laser polarization axes and ε_0 is the envelope of the electric field of the laser pulse. All the calculations presented in this paper were performed with Gaussian laser pulses.

The equation of motion for the angular rotation of the molecule is then given by [5, 17]

$$\ddot{\theta} = -\frac{\alpha_{\text{eff}}}{4I(t)}\varepsilon_0^2 \sin 2\theta - 2\frac{\dot{R}}{R}\dot{\theta} \tag{2}$$

where $\alpha_{\text{eff}} = \alpha_{\parallel} - \alpha_{\perp}$ is the effective polarizability, R is the internuclear separation and $I(t)$ is the time-dependent moment of inertia. For iodine $\alpha_{\text{eff}} = 45.146$ au [18] and for bromine $\alpha_{\text{eff}} = 28.33$ au [19]. The second term in equation (2) is a damping term that leads to a reduced acceleration as the ions move apart. If the molecule does not ionize and dissociate, this term is zero and the molecule continues to rotate even after the laser field is switched off.

In our calculations, we assume that α_{eff} is constant during rotation, ionization and dissociation. The effect of this approximation is discussed more fully in section 3.6.

The calculations presented in this paper assume that the initial rotational velocity of the iodine molecules is zero. We have examined the effect of non-zero initial rotational velocities on the observed angular distributions and find that no significant change in the angular distributions occurs for the rotational velocities expected in a molecular beam with a temperature of ∼10 K (as used in the experiments described in [8]).

The effect of the initial rotational temperature on the degree of alignment has previously been studied experimentally by changing the carrier gas used in the expansion of iodine into the vacuum chamber [23]. With nanosecond alignment pulses at an intensity of $\sim 10^{12}$ W cm^{-2}, it was found that the lower rotational temperature with Ar than with He as the carrier gas resulted in a more localized angular distribution. The initial rotational velocity plays a much less important role with the much faster alignment (due to the much shorter, more intense pulses) described in this paper.

2.2. Dissociative ionization of the neutral molecule

The first step in MEDI is multiphoton ionization of the neutral molecule, followed by its dissociation. This occurs at a laser intensity in the region of 10^{13} W cm^{-2} for iodine and bromine. The effect of the threshold intensity for dissociative ionization on the calculated degree of alignment is discussed in section 3.5.

The over-the-barrier (OTB) threshold for the appearance intensity of I_2^+ and Br_2^+ can be calculated from the shape of the potential energy surfaces of the singly charged molecules, as described in [10]. For iodine, which has an ionization potential of 9.3 eV, this gives a value of 2.3×10^{13} W cm^{-2} at 0°. For bromine, which has a higher ionization potential (10.45 eV), the OTB threshold calculated in this way is 3.8×10^{13} W cm^{-2}. However, these threshold intensities give a much stronger amount of alignment and a shorter optimum alignment time than we observed experimentally [8]. We found the best agreement with our experimental measurements were consistent with a threshold intensity at 0° of 7×10^{12} W cm^{-2} for iodine and 1.1×10^{13} W cm^{-2} for bromine. A multiphoton ionization threshold of 8×10^{12} W cm^{-2} for iodine was measured in [20] with 630 nm radiation. The angular dependences of the threshold intensities were then obtained from the shape of the potentials (equation (4)). Analytical fits to the numerically calculated threshold intensities give

$$\begin{aligned} I_{\text{threshold}(I_2)} &= \frac{2.94 \times 10^{13}}{|\cos\theta|^{1.66} + 3.28} \\ I_{\text{threshold}(Br_2)} &= \frac{5.19 \times 10^{13}}{|\cos\theta|^{1.65} + 3.51}. \end{aligned} \tag{3}$$

The calculations presented throughout this paper use the threshold intensities for formation of I_2^+ and Br_2^+ obtained from these equations.

2.3. Field ionization and Coulomb explosion

Once the molecule has been singly ionized, it starts to dissociate. Following [10], we assume that, for internuclear separations less than 10 au, the ions move apart as if due to the mutual Coulomb repulsion of two ions each with charge $\frac{1}{2}$. Once the internuclear separation is greater than 10 au the I and I^+ fragments are assumed to no longer repel each other. This division of the dynamics into two regions was found to reproduce the observed kinetic energy in this channel [10].

As the molecule flies apart and rotates in the time-dependent laser field, we check whether further ionization is possible. We assume the outer electron in the molecule moves freely in the potential well of the two ion cores. The two-dimensional double-well potential, $V(x, y)$, of a diatomic molecule in a uniform electric field, ε_0, with the two ion cores located at $x = \pm R/2$ can be written as

$$V(x, y) = -\frac{Q/2}{\sqrt{(x + R/2)^2 + y^2}} - \frac{Q/2}{\sqrt{(x - R/2)^2 + y^2}} - \varepsilon_0 x \cos\theta - \varepsilon_0 y \sin\theta. \tag{4}$$

Here, Q is the sum of the charges on the atomic cores. The shapes of the potential well for the I_2^+ molecule for three different values of θ, R and ε are shown in figures 1(*a*)–(*c*). There are, in general, two saddle-points on the potential energy landscape defined by equation (4). If the electron has enough energy, it will leave the ion by travelling over one of these saddle-points. The positions of the saddle-points are found by looking for points where

$$\frac{\partial V(x, y)}{\partial x} = \frac{\partial V(x, y)}{\partial y} = 0. \tag{5}$$

Following [21], we approximate the electron energy, E, as the average of the ionization potentials, E_1 and E_2, of the two ions with charges Q_1, Q_2 where $Q = Q_1 + Q_2$, lowered by the Coulomb potential of the neighbouring ion, $Q_{1,2}/R$

$$E = \frac{(-E_1 - Q_2/R) + (-E_2 - Q_1/R)}{2}. \tag{6}$$

As the ion cores move apart, the central barrier between the two ions becomes higher than the outer barrier on the 'downhill' side of the potential energy landscape. The electron can then become localized on the 'uphill' ion. If this happens, its energy is Stark-shifted upwards by an amount $\Delta E = \frac{1}{2}\varepsilon_0 R \cos\theta$. In figure 1(*a*), the iodine molecular ion is at the equilibrium internuclear separation of 5.04 au and oriented along the polarization axis. In this case, there is no electron localization and no Stark-shift as the central barrier is lower than the outer barrier. Figure 1(*b*) shows the potential wells for the molecule in the same orientation and same electric field strength, but with the ion cores 10 au apart. At this larger internuclear separation, the central barrier has risen higher than the outer barrier. In figure 1(*c*), the molecule is 45° to the polarization axis and has an internuclear separation of 9.54 au. Because the electron is localized, the electron energy is Stark shifted upwards. This lowers the threshold ionization intensity to 1.5×10^{13} W cm^{-2}, compared with 5.8×10^{13} W cm^{-2} for a molecule with the same orientation but at the equilibrium internuclear separation. The internuclear separation where the threshold intensity is lowest is referred to as the 'critical internuclear distance' [10] and is ~10 au in iodine. As the Stark shift is proportional to $\cos\theta$, it is zero when the molecule is perpendicular to the laser field, even though the electron can be localized on one ion.

Figure 1(*d*) shows the threshold intensity for ionization from (I^+, I) to (I^+, I^+) as a function of the internuclear distance for molecules oriented parallel to, at 45° to and perpendicular to the laser electric field. This same result is also shown in figure 3 of [6]. The threshold intensity for ionization is angle-dependent, being lowest for molecules oriented along the laser

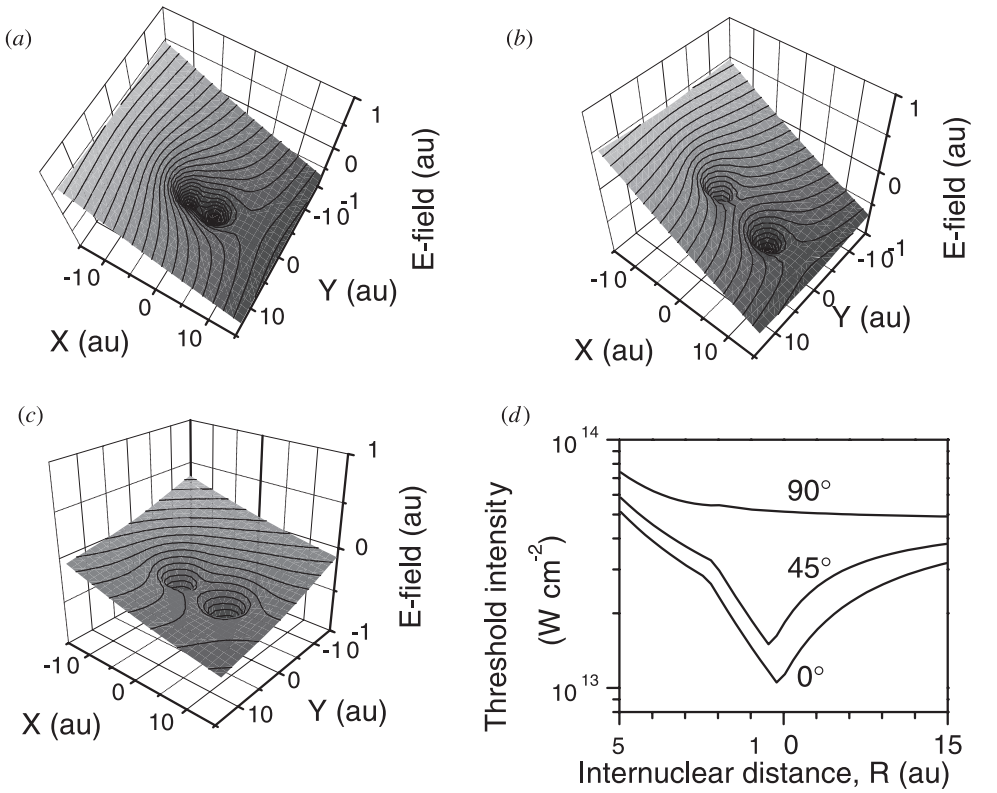

Figure 1. (*a*) Potential energy landscape of an I_2^+ molecule oriented with the internuclear axis parallel to the laser polarization. The molecule is at the equilibrium internuclear separation of 5.04 au and the laser intensity is 5.1×10^{13} W cm^{-2}. (*b*) I_2^+ molecule parallel to the laser polarization. The internuclear separation is 10 au and the laser intensity is again 5.1×10^{13} W cm^{-2}. (*c*) I_2^+ molecule at 45° to the laser polarization. The internuclear separation is 9.54 au and the laser intensity is 1.5×10^{13} W cm^{-2}. (*d*) Threshold intensity for ionization from (I^+, I) to (I^+, I^+) as a function of internuclear separation for molecules oriented at 0°, 45° and 90° to the laser polarization axis.

polarization axis. At small internuclear separations ($\lesssim 8$ au), where the electron leaves the molecule by passing over the outer potential barrier, the outer barrier is furthest from the centre of the molecule when the molecule is parallel to the electric field, and so is lowered more by the electric field. At larger internuclear separations, the electron is localized and the angular dependence of the ionization rate arises primarily because the Stark shift of the electron energy is proportional to $\cos\theta$. This angular dependence of the threshold intensity for over-the-barrier ionization is geometric alignment.

Following further ionization, the molecule Coulomb explodes as the two ion cores repel each other. The equation of motion is given by

$$\ddot{R} = \left(\frac{Q-1}{2}\right)^2 \frac{1}{MR^2} \tag{7}$$

where M is the mass of the molecule and the net charge on the molecule is $Q-1$. Equation (7) assumes that the molecular charge is split equally between the two ions. In the equation of motion, we allow the molecules with asymmetric charge states to have non-integer charges on each ion for the purposes of calculating the radial motion due to Coulomb explosion.

The field-ionization Coulomb explosion model assumes that the only charge channels that can occur are ($I_2^{2n+} \rightarrow I^{n+}$, I^{n+}) or ($I_2^{(2n+1)+} \rightarrow I^{n+}$, $I^{(n+1)+}$). However, charge asymmetric dissociation channels ($I_2^{2n+} \rightarrow I^{(n+1)+}$, $I^{(n-1)+}$) have also been observed experimentally with significant branching ratios [8, 22].

2.4. Angular distributions and focal volume averaging

For each intensity and pulse-length, we calculated the trajectories of a set of molecules with initial angles with respect to the laser polarization axis varying from 0° to 90° in one degree steps. The angular distributions are calculated from the angle between each molecule and the polarization axis at the end of the laser pulse, once the angular velocity has returned to zero. The angular distribution is independent of the azimuthal angle, ϕ, around the laser polarization axis. The number of ions with initial angle θ to $\theta + d\theta$ is proportional to $\sin\theta\, d\theta$. In spherical coordinates, the size of a volume element is equal to $dv \sin\theta\, d\phi\, d\theta$, where v is the ion velocity. Integration of the 3D velocity distribution $P(v, \theta, \phi)$ over v and ϕ leads to a determination of $P(\cos\theta)$. Throughout this paper, we plot $P(\cos\theta)$, which is constant for an isotropic angular distribution.

The final angular distributions were averaged over the intensity distribution in the focal volume, by taking the weighted sum of approximately 200 iso-intensity shells. To allow comparison with the experimental results reported in [8], we assume a loosely focused Gaussian beam intersecting a narrow molecular beam so that the laser intensity does not vary along the width of the molecular beam. If the entire chamber is filled with gas, it would then be more appropriate to use equations for the full focal volume distribution [6]. The angular distributions obtained in these two cases can be very different, due to the much larger low-intensity region sampled when the entire focal volume is considered.

As a measure of the width of the angular distribution, we use the full-width at half maximum of the angular distribution (FWHM) calculated assuming the distribution is a Gaussian centred at 0°. The width of distribution is calculated using

$$\mathrm{FWHM} = 2\sqrt{\pi \ln 2}\frac{\int_0^{90} \theta F(\theta)\, d\theta}{\int_0^{90} F(\theta)\, d\theta}. \tag{8}$$

It is difficult to use only one parameter to characterize an angular distribution, which may consist of multiple peaks. Equation (8) only gives meaningful results for angular distributions peaked at 0°. We chose to use this formula to allow direct comparison with the experimental measurements of Rosca *et al* [8].

3. Results

3.1. No dynamic alignment

In order to be able to evaluate the degree of dynamic alignment occurring, we first need to understand the angular distributions that arise in the case of geometric alignment alone.

If there is no dynamic alignment and we assume an angle-dependent ionization rate only, the angular distribution of the *total* ion signal depends on intensity but not pulse duration. This is because whether a molecule ionizes or not depends only on whether the intensity is high enough at its original orientation. Above the intensity at which all the molecules ionize, the angular distribution just has an increasing uniform background (figure 2(*a*)). The width of the angular distribution (calculated using equation (8)) increases from $\sim 84°$ at an intensity of

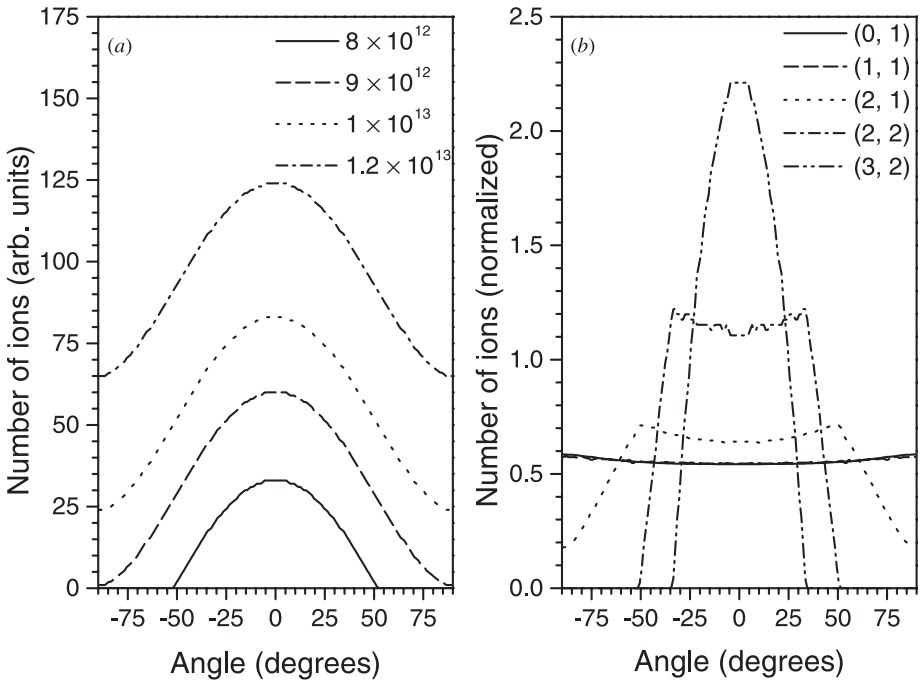

Figure 2. (*a*) The angular distribution of all dissociated ions for a range of intensities with a 100 fs laser pulse. Geometric alignment alone is considered. (*b*) Angular distributions of ions in each charge channel from $I + I^+$ (0, 1) to $I^{3+} + I^{2+}$ (3, 2), with geometric alignment alone. The laser pulse is 100 fs long and the peak laser intensity is 1.25×10^{14} W cm^{-2}. The number of ions in each channel has been normalized.

9×10^{12} W cm^{-2} (the lowest intensity where molecules at 90° to the polarization axis can be ionized) to $\sim 130°$ above 10^{14} W cm^{-2}.

The width of the angular distributions for each charge channel decreases with the charge of the channel (figure 2(*b*)). The most highly charged ions are peaked along the polarization axis, where the threshold intensity for these charge states is lower. The lowest charge channels have distributions that are lower along the polarization axis, where the ions have been ionized to higher charge states. (Due to the large numbers of ions in the (0, 1) and (1, 1) channels produced in the low-intensity regions of the focus in figure 2(*b*), the angular distributions of these channels are only very slightly depleted at the centre). The intermediate charge states have angular distributions peaked at intermediate angles as those molecules at large angles are in lower charge states, and those at small angles have been ionized to higher charge states. Experimental measurements by this group [8] have also shown that, with 80 fs pulses, the angular distribution for low charge channels has a minimum along the polarization axis, indicating depletion due to ionization to higher charge channels, but the highest charge states are peaked along the polarization axis.

Although the angular distribution summed over all ions is independent of pulse-length if geometric alignment alone occurs, the angular distributions and branching ratios of individual channels can change with pulse-length (as do the kinetic energies of the ions [10]). The highest charge states are observed at intermediate pulse durations of a few hundred femtoseconds. For these pulse durations, the molecule reaches the critical internuclear distance ($\sim$10 au for iodine) near the peak of the laser pulse so enhanced ionization occurs.

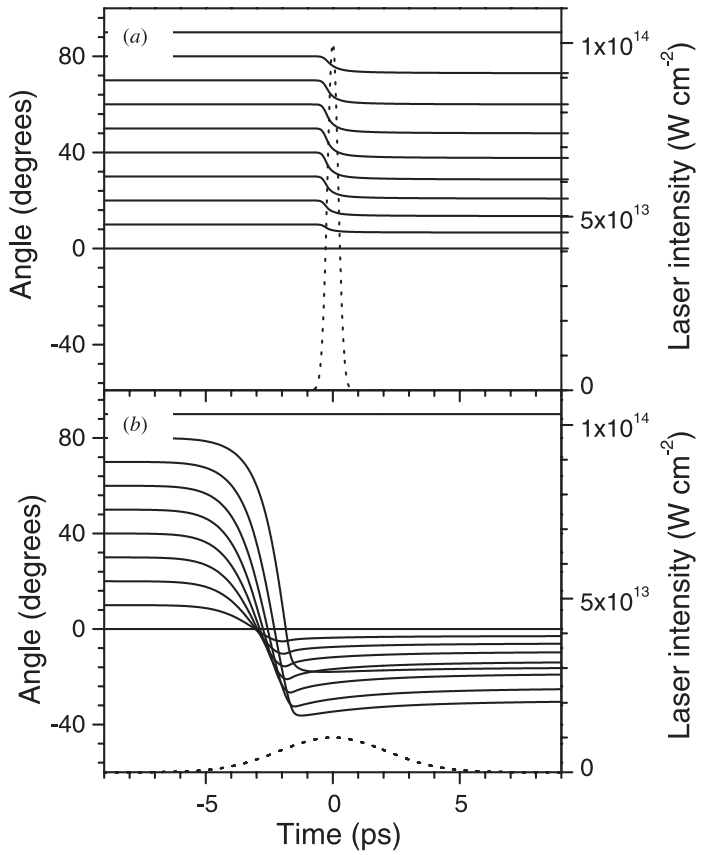

Figure 3. Calculated trajectories for ions with a range of initial angles for: (*a*) a 500 fs pulse with a peak intensity of 1×10^{14} W cm^{-2}; and (*b*) a 5 ps pulse with peak intensity 1×10^{13} W cm^{-2}. The dotted curves show the intensity of the laser pulse.

3.2. Ion trajectories with dynamic alignment

When the dynamic rotation of the molecules by the laser field is included in the calculation, the length of the laser pulse has a major influence on the degree of alignment. Calculated trajectories for ions with a range of initial angles irradiated by a 500 fs or 5 ps pulse with the same energy are shown in figure 3. With the 500 fs pulse (figure 3(*a*)), the molecules are rotated slightly towards the polarization axis by the laser field early in the laser pulse. However, the molecules ionize and start to dissociate ~ 500 fs before the peak of the laser pulse and, at this point, the angular velocity drops rapidly to zero due to conservation of angular momentum (equation (2)). When the molecules are irradiated by the lower intensity 5 ps pulse, dissociation does not occur until ~ -1.8 ps. By this time, most molecules have had time to cross the polarization axis and the final angles are distributed close to the laser polarization axis.

The angular distributions obtained with short pulses ($\lesssim$100 fs) are similar to those obtained from geometric alignment alone (compare figure 4(*a*) with figure 2(*b*)). As the pulse-length increases, the distributions narrow, first to sharp peaks with a shoulder (figure 4(*b*)) and then the size of the shoulder decreases (figure 4(*c*)). Two contradictory factors affect the relative widths of the charge channels. Firstly, the highest charge-state produced tends to be closely

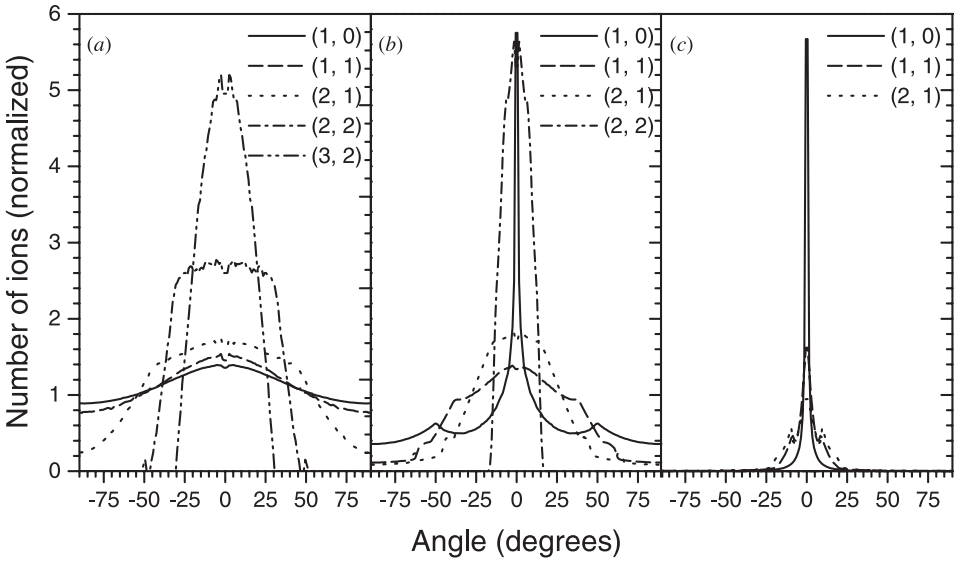

Figure 4. Angular distributions of ions in each charge channel with both geometric and dynamic alignment. The length of the laser pulse is (*a*) 100 fs, (*b*) 1 ps and (*c*) 3 ps. In each case, the peak laser intensity is 1.25×10^{14} W cm^{-2}. The number of ions in each channel has been normalized.

aligned due to geometric effects because the highly charged ions are produced close to the polarization axis. (See, for example, the (2, 2) channel in figure 4(*b*).) Secondly, low charge states tend to have narrow angular distributions when dynamic alignment dominates because (as we explain in the following section) ions from the low-intensity regions of the focus align more.

Experimentally, we observed that the angular distributions change from short to long pulses in qualitatively the same way as described here. With the shortest pulses used (80 fs), the angular distributions were broad (FWHM of 90° to 120°) and the maximum was away from 0° due to depletion of ions to higher charge states (figure 2 of [8]). With ~ 3 ps laser pulses, the angular distribution was sharply peaked along the laser polarization axis with FWHM of 10° to 40°, and no ions were present perpendicular to the laser polarization (figure 6 of [8]).

3.3. Intensity scaling

The behaviour of the width of the angular distribution with increasing intensity is complicated by several competing effects. For a given angle, the initial amount of rotation increases with increasing intensity because the angular acceleration is proportional to the square of the electric field ($\ddot{\theta} \propto E^2$). However, molecules that experience higher laser intensities dissociate earlier on in the pulse. With the Gaussian laser pulses used in these calculations, molecules that experience higher intensities can end up less aligned. Figure 5 shows the final angles of molecules with initial angles of 20°, 40°, 60° and 80° as a function of laser intensity. The molecules irradiated with the lowest intensity laser pulses undergo the most rotation.

When geometric alignment alone is considered, the width of the angular distribution for all ions increases with laser intensity. The intensity dependence is the same for all pulse-durations as whether or not a molecule reaches the first ionization stage depends only on the angle it makes with the laser polarization axis and the peak intensity it experiences. When dynamic

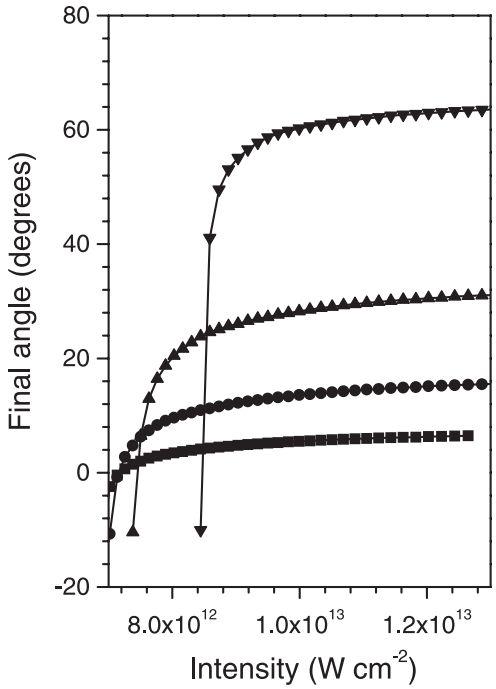

Figure 5. Final angles reached by molecules with initial angles of 20° (squares), 40° (circles), 60° (up triangles) and 80° (down triangles) as a function of laser intensity. For each data point plotted, the laser pulse was 1500 fs long and the charge channel reached was (0, 1).

alignment is included in the model, the intensity dependence is different for different pulse durations, as shown in figure 6. For short (∼100 fs) pulses, the intensity dependence is close to that for geometric alignment alone, showing that selective dissociative ionization dominates over dynamic alignment. For longer pulses (∼ 5 ps), dynamic alignment dominates and the angular distribution is much narrower and varies less with laser intensity. In this case, the majority of alignment occurs before the molecule starts to dissociate. As the laser intensity is increased, the dissociative ionization threshold moves earlier and earlier in the laser pulse so that the net amount of alignment does not necessarily increase.

We have observed these trends experimentally as shown in figure 7 of [8]. We observe that for intensities above $\sim 6 \times 10^{13}$ W cm^{-2} the width of the angular distribution increases with intensity because, through the mechanism outlined above, the dynamic alignment decreases and the alignment is dominated by geometric effects. This effect was also seen by Posthumus and co-workers, who observed an increase in FWHM with increasing intensity for iodine molecules irradiated with 50 fs laser pulses at intensities between 10^{13} and 10^{15} W cm^{-2} [6], consistent with geometric alignment. For longer pulses, we observed progressively narrower angular distributions and the angular distributions vary less with laser intensity, in qualitative agreement with figure 6. At a fixed intensity, the width of the angular distribution decreases with increasing pulse duration, indicating that dynamic alignment occurs. For example, with a fixed intensity of 2.65×10^{13} W cm^{-2}, the FWHM of the angular distribution of the $I^+ + I^+$ channel decreases from $54.3 \pm 0.9°$ with 3 ps pulses to $25.2 \pm 0.8°$ with 1 ps pulses.

Experimentally, we observed a decrease in FWHM with intensity for intensities below $\sim 3 \times 10^{13}$ W cm^{-2} [8], which is not reproduced by the calculations. This is because, under

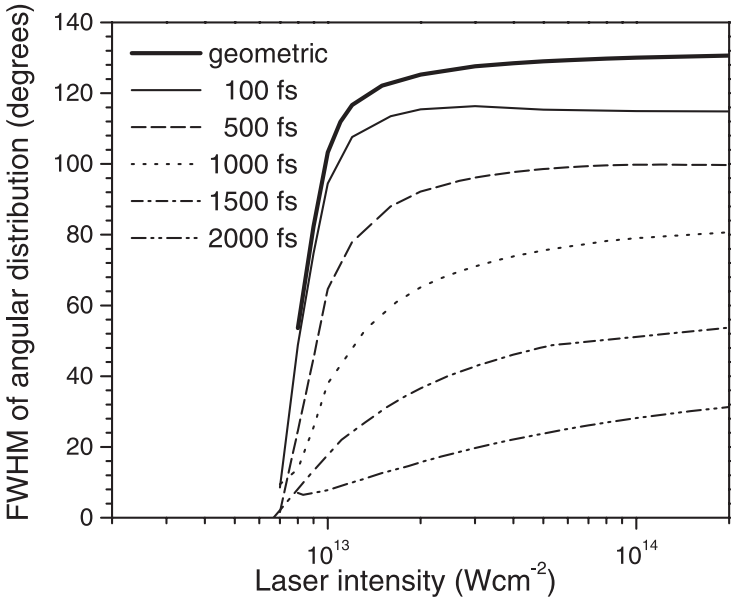

Figure 6. The FWHM of the angular distribution of all ions plotted as a function of the laser intensity for geometric alignment alone (thick full curve) and including dynamic alignment for 100, 500 fs, 1, 1.5 and 2 ps pulses.

these conditions, we are below the threshold intensity for over-the-barrier field ionization and are no longer in the regime treated by this model. At these lower intensities, dynamic alignment dominates and the increase in alignment with intensity reflects the increased alignment forces when the intensity is increased. In nanosecond-pump femtosecond-probe experiments (e.g. [23]), the degree of alignment increases with the intensity of the nanosecond laser pulse, so long as it remains below the ionization threshold.

3.4. Variation with pulse duration

Figure 7 shows the variation of the FWHM of the angular distribution with pulse-length at constant pulse energy (or fluence) for the total ion signal (figure 7(*a*)) and for each individual dissociative ionization channel (figure 7(*b*)). When dynamic alignment is included, the angular distributions narrow with increasing pulse-length, reaching a minimum width of $\sim 10^{\circ}$ at a pulse-length of 3 ps before broadening and then narrowing again. The initial narrowing of the angular distributions as the pulse-length increases is due to the ionization threshold being reached closer to the peak of the laser pulse. As the pulse-length increases beyond the optimum, the molecules rotate too much and overshoot the polarization axis (as in figure 3(*b*)) before being ionized. This results in a broadening of the angular distribution. If the pulse-length is increased still further, the angular distribution will narrow again as the molecules oscillate and return to the polarization axis before ionization. The optimum pulse-length is longer for higher energy pulses because the ionization point occurs earlier in the laser pulse. This means that longer pulses are required to give the molecule time to rotate to the polarization axis before the intensity rises past the ionization threshold.

Figure 7(*b*) shows that the highest charge channel produced at a given pulse length tends to be the most strongly aligned. This is because more aligned molecules reach higher charge states

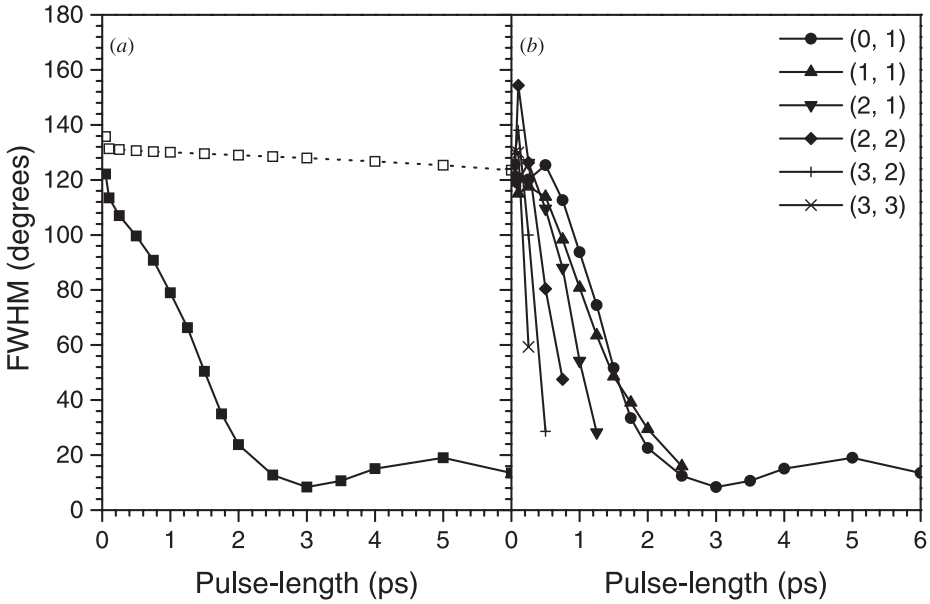

Figure 7. FWHM with pulse duration at fixed fluence of 100 J cm^{-2}. (*a*) For all ions at fluences of 100 J cm^{-2} with both geometric and dynamic alignment (full curves, full squares) and with geometric alignment alone (dotted curves, open squares). (*b*) For each charge channel from (0, 1) to (3, 3) with both geometric and dynamic alignment.

due to the lowered ionization thresholds for molecules oriented close to the laser polarization axis.

With geometric alignment alone, the width of the angular distribution for all ions is independent of pulse-length at constant intensity. At a constant fluence of 100 J cm^{-2}, the width of the distribution decreases from $\sim$135° to $\sim$130° as the pulse length is increased from 50 fs to 6 ps, due to the drop in intensity. If the angular distributions of the individual charge channels are analysed, we find that the highest charge channels narrow as the pulse-length increases (as the intensity drops, these high charge states can only be produced close to the polarization axis). In this case, the low charge channels will be depleted about the polarization axis (as described in section 3.1).

The results of our numerical calculations are compared with those measured experimentally in figure 11 of [8]. The experimental results show good agreement with the calculations and confirm that dynamic alignment narrows the angular distributions for pulses longer than $\sim$ 500 fs. In particular, we experimentally observe a decrease in FWHM with increasing pulse duration for pulse lengths below 3 ps, followed by a broadening of the angular distribution as the pulse-length increases. We also observe that higher charge channels are more tightly aligned at a given pulse duration, in agreement with our calculations.

3.5. Effect of changing molecular parameters

In order to understand how the molecular parameters affect the rate at which a molecule aligns, we have examined the effect of changing the polarizability, mass and dissociative ionization threshold (figure 8(*a*)). Decreasing α_{eff} simply reduces the angular acceleration, with the obvious result that the ions are less aligned. Decreasing both the mass and α_{eff} but keeping

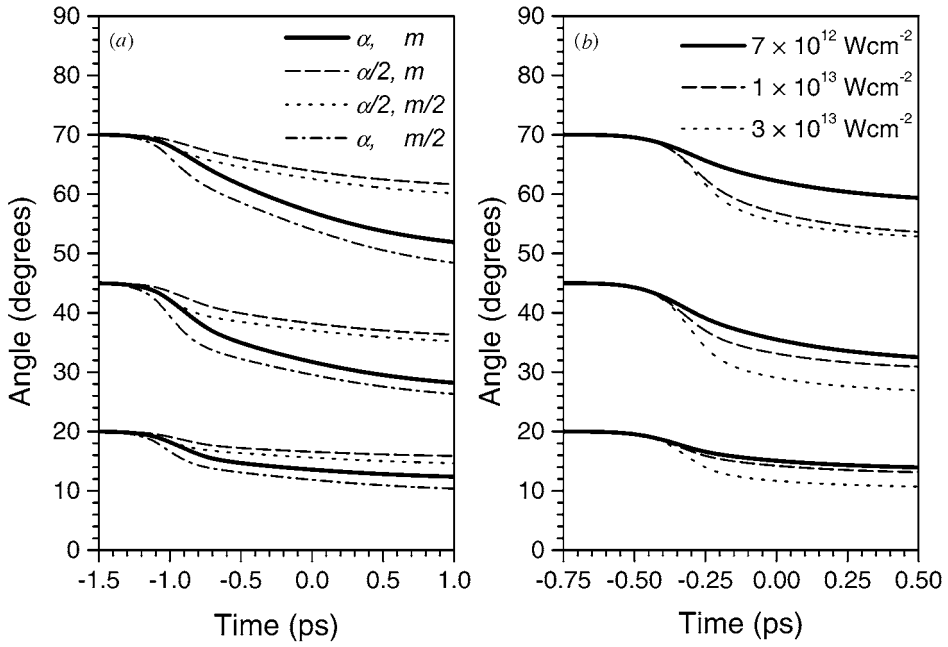

Figure 8. Trajectories for ions with three different initial angles (20°, 45° and 70°) for 500 fs laser pulses with a peak intensity of 2×10^{14} W cm^{-2}. (*a*) Mass or polarizability changed. Thick full curves, iodine ions ($\alpha = \alpha_{\text{iodine}} = 45.146$ au, $m = m_{\text{iodine}} = 126.9$); broken curves, $\alpha = \alpha_{\text{iodine}}/2$; chain curves, $m = m_{\text{iodine}}/2$; dotted curves, $\alpha = \alpha_{\text{iodine}}/2$, $m = m_{\text{iodine}}/2$. (*b*) Trajectories with three different threshold intensities: 7×10^{12}, 1×10^{13} and 3×10^{13} W cm^{-2}.

their ratio the same means that the first term in equation (2) remains the same as it depends on α_{eff}/mass. Therefore, before dissociation, the molecules with the same α_{eff}/mass ratio follow the same path. However, once the molecule is ionized, the one with the lower mass will dissociate more rapidly leading to a more abrupt end to its rotation and less alignment. A molecule with low mass but high α_{eff} experiences the strongest alignment as the rotation of the undissociated ion is more rapid, even though the deceleration due to the Coulomb explosion is also faster.

The intensity at which a molecule ionizes and begins to dissociate is an important factor in determining the amount of alignment. The effect of reducing the threshold intensity at which the ions begin to dissociate is to reduce the amount of alignment (figure 8(*b*)). Rotation slows once the molecule begins to dissociate, and so a molecule that dissociates earlier in the laser pulse will have experienced less rotation. We find that the optimum pulse-length for alignment is longer for a lower threshold (figure 9(*a*)). For example, for pulses with a constant fluence of 100 J cm^{-2}, the optimum pulse-length is 1 ps for a threshold intensity of 3×10^{13} W cm^{-2}. If the threshold intensity is dropped to 1×10^{13} W cm^{-3}, the optimum pulse-length increases to 2 ps and with a threshold of 7×10^{12} W cm^{-2}, the optimum pulse-length is 3 ps.

From these arguments, molecules that align most strongly will have (a) a high-α/mr^2 ratio and in order to maximize the amount of alignment of the neutral molecule and (b) a high ionization potential (as most alignment occurs before the molecule ionizes and begins to dissociate). Table 1 compares the properties of I_2 and Br_2. The bromine molecule has a higher ionization potential and α/mr^2, but a lower mass. We have compared the degree of alignment observed in Br_2 to that in I_2 and find that bromine aligns much faster, with the optimum pulse-

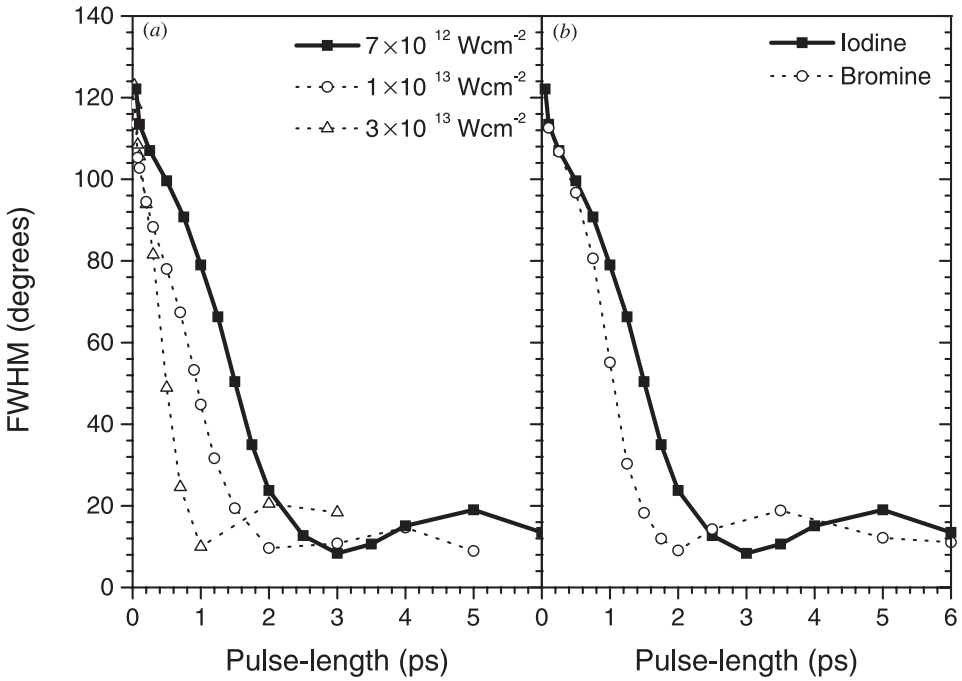

Figure 9. (*a*) FWHM with pulse duration for three different threshold intensities: 7×10^{12}, 1×10^{13} and 3×10^{13} W cm^{-2}. (*b*) FWHM of distribution as a function of pulse-length for iodine (full curve, full squares) and bromine (dotted curve, open circles). The threshold intensity here is 7×10^{12} W cm^{-2} for iodine and 1.1×10^{13} W cm^{-2} for bromine. In both (*a*) and (*b*) the product of the pulse-length and intensity is kept constant at 100 J cm^{-2}.

Table 1. Comparison of molecular parameters for I_2 and Br_2.

	Iodine	Bromine
α (au)	45.146 [18]	28.33 [19]
Mass (m)	126.9	79.904
Internuclear separation (au)	5.04	4.31
Molecular I_P (eV)	9.31	10.54
Threshold intensity at 0° (W cm^{-2}) (equation (3))	6.9×10^{12}	1.15×10^{13}
Threshold intensity at 90° (W cm^{-2}) (equation (3))	9.0×10^{12}	1.48×10^{13}

length being 2 ps for Br_2 compared with 3 ps for I_2 (figure 9(*b*)). This is in agreement with our experimental measurements shown in figure 11 of [8]. This suggests that the higher α/mr^2 and ionization potential are more important than the mass. While the mass affects the degree of alignment after dissociation, the other two factors affect how the undissociated molecule aligns.

3.6. Change in polarizability on dissociation

We assume in our model that the value of the effective polarizability remains constant throughout the interaction. It is obvious that this is an approximation for several reasons. First, the values of $\alpha_\parallel$ [24] and α_{eff} [19] increase with elongation of the molecule. For example, for bromine $\alpha_{\text{eff}} = 28.33$ at the equilibrium distance of 4.31 au and 30.90 at just 4.40 au [19].

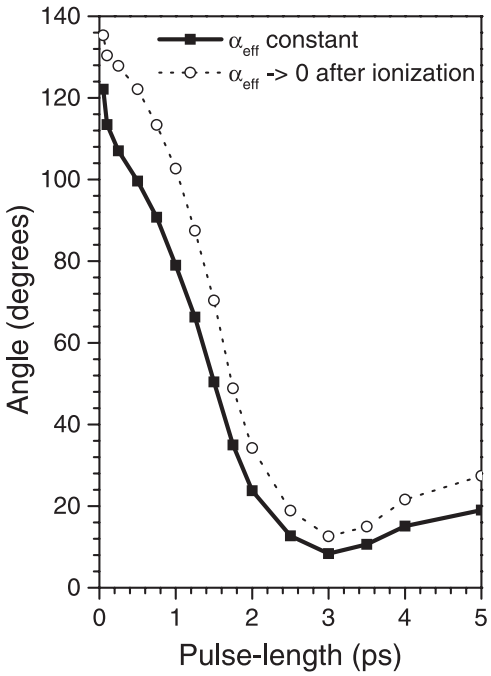

Figure 10. FWHM of angular distribution as a function of pulse-length for all dissociated ions. The molecule is iodine and the fluence is 100 J cm^{-2}. Full curve with full squares: α_{eff} constant throughout. Dotted curve with circles: α_{eff} set to zero immediately upon dissociation.

This is an increase of nearly 10% for a 2% increase in bond length. Secondly, α_{eff} decreases with increasing charge and can even become negative in some states [5]. Thirdly, α_{eff} differs from the zero-field value even in the ground state in intense fields [25] and, finally, the electron localization that occurs at the critical internuclear distance must reduce the polarizability [5].

To estimate the degree of the error introduced by this approximation, we have performed some calculations where α_{eff} is set to zero immediately upon ionization (figure 10). The effect of this is to bring the angular velocity more rapidly back to zero when the molecule starts to dissociate. We find that, averaged over the focal volume distribution, the effect of this is to increase the width of the angular distribution by $\sim 20^\circ$ for short (<1 ps) pulses and $\sim 5^\circ$ for long (> 2 ps) pulses. This means that, in this model, at short pulse-lengths a significant fraction of the rotation takes place while the molecule is dissociating. However, for longer pulses more rotation occurs before dissociation, so the fraction of rotation that occurs during dissociation is smaller.

4. Discussion

4.1. Geometric versus dynamic alignment

Several experiments [6, 7] have used the intensity scaling of the angular distribution to attempt to distinguish between dynamic and geometric alignment. For geometric alignment (angle-dependent ionization), the FWHM and the number of ions perpendicular to the laser polarization will increase with intensity as molecules progressively closer to 90° to the laser polarization become able to dissociate. The signature of dynamic alignment (rotation of the

molecules) was predicted in [6, 7] to be a decrease in the FWHM of the distribution with increasing intensity, as the acceleration of the molecules is proportional to the square of the electric field. A lack of fragments perpendicular to the laser polarization at all intensities was also predicted.

We find, however, that dynamic alignment can also result in an angular distribution that broadens as the intensity increases, because the majority of alignment takes place on the leading edge of the pulse before the molecule dissociates. As the intensity increases, the energy in the leading edge of the pulse below the dissociation threshold actually decreases for a Gaussian pulse. Our calculations suggest that to distinguish between geometric and dynamic alignment it is necessary to vary the pulse-length. The cleanest test is to measure the angular distribution of all ions as a function of pulse-length, keeping the intensity constant. If geometric alignment alone takes place the angular distribution summed over all fragment charge states will be independent of pulse-length, within the over-the-barrier ionization model. However, if dynamic alignment takes place the angular distribution will narrow as the pulse-length increases.

5. Conclusions

We have calculated the angular distributions of the ions produced by multi-electron dissociative ionization of iodine and bromine molecules, using a two-dimensional field-ionization Coulomb explosion model including dynamic rotation of the molecule in the laser field. We have investigated the dependence of the degree of alignment on laser intensity and pulse-length, as well as on molecular parameters such as mass, polarizability and dissociative ionization threshold intensity.

We find that the majority of dynamic alignment occurs on the leading edge of the laser pulse at low intensities before the laser intensity reaches the dissociative ionization threshold. This makes the degree of alignment sensitive to the value of the dissociative ionization threshold, with the optimum pulse-length for alignment being longer for a lower ionization threshold.

With short pulses ($<$100 fs), the anisotropy of the fragment ions is primarily due to selective dissociative ionization of molecules aligned close to the polarization axis (geometric alignment). For pulses longer than $\sim$1 ps, the observed angular distributions are dominated by dynamic rotation of the molecules. Angular distributions as narrow as 10° FWHM can be achieved with long pulses.

Depletion close to the polarization axis of the angular distributions of the lowest charge channels produced is an indication that geometric alignment dominates. Increased alignment of all charge channels as the pulse-length increases is an unambiguous sign that the molecules are forced into alignment with laser field.

Acknowledgments

This work is part of the research programme of the 'Stichting voor Fundamenteel Onderzoek der Materie (FOM)', which is financially supported by the 'Nederlandse organizatie voor Wetenschappelijke Onderzoek (NWO)'. ES is supported by a Marie Curie Individual Fellowship from the European Community Fifth Framework Training and Mobility of Researchers programme. We would like to thank Celine Nicole and Arjan Houtepen for helpful discussions.

References

[1] Cornaggia C, Lavancier J, Normand D, Morellec J, Agostini P, Chambaret J P and Antonetti A 1991 *Phys. Rev.* A **44** 4499
[2] Dietrich P, Strickland D T, Laberge M and Corkum P B 1993 *Phys. Rev.* A **47** 2305
[3] Normand D, Lompré L A and Cornaggia C 1992 *J. Phys. B: At. Mol. Opt. Phys.* **25** L497
[4] Posthumus J H, Plumridge J, Frasinski L J, Codling K, Langley A J and Taday P F 1998 *J. Phys. B: At. Mol. Opt. Phys.* **31** L985
[5] Ellert C and Corkum P B 1999 *Phys. Rev.* A **59** R3170
[6] Posthumus J H, Plumridge J, Thomas M K, Codling K, Frasinski L J, Langley A J and Taday P F 1998 *J. Phys. B: At. Mol. Opt. Phys.* **31** L553
[7] Banerjee S, Ravindra Kumar G and Mathur D 1999 *Phys. Rev.* A **60** R3369
[8] Rosca-Pruna F, Springate E, Offerhaus H L, Krishnamurty M, Farid N, Nicole C and Vrakking M J J 2001 *J. Phys. B: At. Mol. Opt. Phys.* **34** 4919
[9] Codling K, Frasinski L J and Hatherley P A 1989 *J. Phys. B: At. Mol. Opt. Phys.* **22** L321
[10] Posthumus J H, Giles A J, Thompson M R and Codling K 1996 *J. Phys. B: At. Mol. Opt. Phys.* **29** 5811
[11] Friedrich B and Herschbach D 1995 *Phys. Rev. Lett.* **74** 4623
[12] Dion C M, Keller A, Atabek O and Bandrauk A D 1999 *Phys. Rev.* A **59** 1382
[13] Kramer K H and Bernstein R B 1965 *J. Chem. Phys.* **42** 767
[14] Loesch H J and Remscheid A 1990 *J. Chem. Phys.* **93** 4779
[15] Larsen J J, Hald K, Bjerre N, Stapelfeldt H and Seideman T 2000 *Phys. Rev. Lett.* **85** 2470
[16] Verlotta R, Hay N, Mason M B, Castillejo M and Marangos J P 2001 *Phys. Rev. Lett.* **87** 183901
[17] Banerjee S, Mathur D and Ravindra Kumar G 2001 *Phys. Rev.* A **63** 045401
[18] Callahan D W, Yokozeki A and Muenter J S 1980 *J. Chem. Phys.* **72** 4791
[19] Archibong E F and Thakkar A J 1993 *Chem. Phys. Lett.* **201** 485
[20] Strickland D T, Beaudoin Y, Dietrich P and Corkum P B 1992 *Phys. Rev. Lett.* **68** 2755
[21] Posthumus J H, Frasinski L J, Giles A J and Codling K 1995 *J. Phys. B: At. Mol. Opt. Phys.* **28** L349
[22] Gibson G N, Li M, Guo C and Nibarger J P 1998 *Phys. Rev.* A **58** 4723
[23] Sakai H, Safvan C P, Larsen J J, Hilligsøe K M, Hald K and Stapelfeldt H 1999 *J. Chem. Phys.* **110** 10 235
[24] Kolos W and Wolniewicz L 1967 *J. Chem. Phys.* **46** 1426
[25] Ravindra Kumar G, Gross P, Safvan C P, Rajgara F A and Mathur D 1996 *J. Phys. B: At. Mol. Opt. Phys.* **29** L95